

DESIGN AND OPERATION OF A BUNCHED-BEAM, PHASE-SPREAD MEASUREMENT

J. D. Gilpatrick, H. Marquez, J. Power, and V. Yuan
 Los Alamos National Laboratory
 Los Alamos, NM 87545

Abstract

A bunch-length monitor system has measured the relative changes in the temporal beam-bunch length of an 2.5 MeV H⁻ beam. This system includes a noninterceptive electromagnetic probe, associated RF-processing electronics, and a system-software algorithm. The probe is an axially-symmetric capacitive pickup with output signals proportional to the bunched-beam image currents traveling through its bore. The RF electronics processes the beam-induced signal to obtain the ratio of its fundamental and fifth-harmonic Fourier components and provides a time-varying output voltage proportional to the phase length of the beam bunch. This paper reviews the measurement hardware, software algorithm, and operational experience.

Introduction

During early experiments, the Ground Test Accelerator (GTA) consisted of an injector, a low-energy beam transport, a radio frequency quadrupole (RFQ), and a beam characterization platform[1]. One of the measurement systems implemented on the beam-characterization platform measures the real-time phase spread of the 2.5-MeV H⁻ bunched beam. The measurement design goal was to provide a wide-bandwidth noninterceptive method by which the beam phase spread is resolved to within ±1° of phase. The method chosen to achieve this goal recognizes that as a beam distribution becomes longer in time, the corresponding width of its frequency-domain distribution decreases. This width is measured by comparing the fundamental Fourier component amplitude (i.e., bunching frequency) with a higher-harmonic-component amplitude. As the beam bunch increases in length, so does the ratio of the fundamental-to-higher-harmonic component amplitudes. As would be expected, the amplitude ratio is dependent on both the width and shape of the beam bunch. This shape dependency reduces the technique's overall accuracy without reducing its resolution. In order to calibrate this ratio phase-spread measurement, it was compared with a phase projection of the longitudinal emittance measured by another technique[2]. Measurements were performed by varying the RFQ cavity voltage which results in varying beam-bunch lengths. The separately-measured phase projection and ratio phase-spread data were then compared as a function of cavity power.

Measurement System Description

The ratio-based phase-spread measurement system consists of three components: a capacitive probe whose output signal depends on the beam-intensity distribution size and shape, associated electronics that process the ratio of the fundamental- and higher-harmonic power components, and an

algorithm that converts the electronics output signals to a voltage proportional to phase spread. The algorithm also linearizes the response of the probe and electronics. Figure 1 shows the electrical model of the capacitive probe, which consists of two concentric rings. The inner ring, of inside radius of 7.5 mm and length of 2 mm, is terminated with Z_C at the bottom of the larger grounded outer ring.

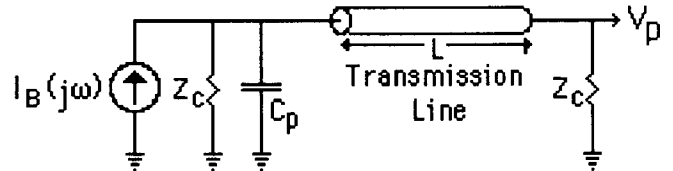


Fig. 1 The capacitive-probe equivalent-circuit model includes the contributions of the beam current, probe capacitance, and cable attenuation.

The signal is extracted from the top of the inner ring through a coaxial connection. Generally, assuming a Gaussian distributed beam, the beam image-charge on the beam tube (without low beam-velocity effects) is

$$\rho(z,t) = -\frac{\theta_0}{2\pi} \frac{eN}{\sqrt{2\pi}\sigma} e^{-\frac{(\beta ct - z)^2}{2\sigma^2}} \quad (1)$$

where $\rho(z,t)$ is the beam charge distribution, eN the total charge per bunch, θ_0 is the subtended angle of the probe (typically 2π), σ is the rms bunch length, and βc is the beam velocity. The beam image current induced on the inner capacitive probe ring, Eq. (3), is the integral of $\rho(z,t)$ in the z -dimension and the derivative in time where τ is the rms bunch temporal length,

$$i_B(t) = -\frac{eN\theta_0}{\sqrt{2\pi}\tau} \left[e^{-\frac{t^2}{2\tau^2}} - e^{-\frac{(t-L/bc)^2}{2\tau^2}} \right], \quad (2)$$

and L is the length of the probe. The beam-induced output voltage, $V_p(j\omega)$, from the probe and transmission line is

$$V_p(j\omega) = \sigma(j\omega) \frac{I_B(j\omega)}{\sqrt{2}} \frac{Z_C}{1 + j\omega Z_C C_p} \frac{1}{I_0\left(\frac{\omega R}{\beta\gamma c}\right)} \frac{2I_1\left(\frac{\omega R}{\beta\gamma c}\right)}{\left(\frac{\omega R}{\beta\gamma c}\right)} \quad (3)$$

where C_p is the probe capacitance, Z_C is the characteristic impedance of the transmission lines and the input impedance of the processing electronics and σ is the cable attenuation[3]. The I_0 and I_1 terms are the zero and first-order Bessel functions that describe the low beam-velocity effects of the beam image-current longitudinal distribution

*Work supported and funded by the US Department of Defense, Army Strategic Defense Command, under the auspices of the US Department of Energy.

due to the probe radius, R , and the diffuse beam radius, r , respectively[4].

The processing-electronics block diagram is shown in Fig. 2. The signal is split and fed to two downconverters, one for the fundamental frequency component, F_0 , of 425 MHz and one for the 2125-MHz component (fourth harmonic).

The choice of this harmonic was dictated by the necessity to balance dynamic range with resolution. The intermediate frequency (IF) signals from the downconverter are then fed to a circuit which takes the difference between the logarithms of the two components (i.e., the ratio of the two components' signal-powers). Finally, an antilogarithm is taken so that the output voltage is proportional to the ratio of the two components' signal amplitudes.

The software algorithm converts the electronics antilogarithm output to a voltage proportional to the rms bunch phase length. Figures 3 a and b graph two calculated quantities as a function of rms bunch phase length for a Gaussian-distributed beam. Figure 3a shows the input signal power of the two components and shows the expected processing-electronics antilogarithm output for the power levels shown in Fig. 3a. The capacitive-probe signal power estimates shown in Fig. 3a were generated by an equation similar to Eq. (3). Offset and gain term errors from this equation were corrected during the calibration of this measurement and substituted into a software algorithm. A calculation of the probe signal powers using Eq. (3) showed agreement with measured beam-signal powers for the fundamental and fourth harmonic components to within a few dB. The software algorithm takes the form of a polynomial least-squares fit to the loci in Fig. 3b and is

$$\phi_{rms}(t) = av_0^5(t) + bv_0^4(t) + cv_0^3(t) + dv_0^2(t) + ev_0(t) + \phi_0 \quad (4)$$

where ϕ_{rms} is the rms phase length of the Gaussian-distributed beam bunch, V_0 is the electronics antilogarithm output-voltage, and ϕ_0 , a, b, c, d and e are the coefficients of the polynomial fit.

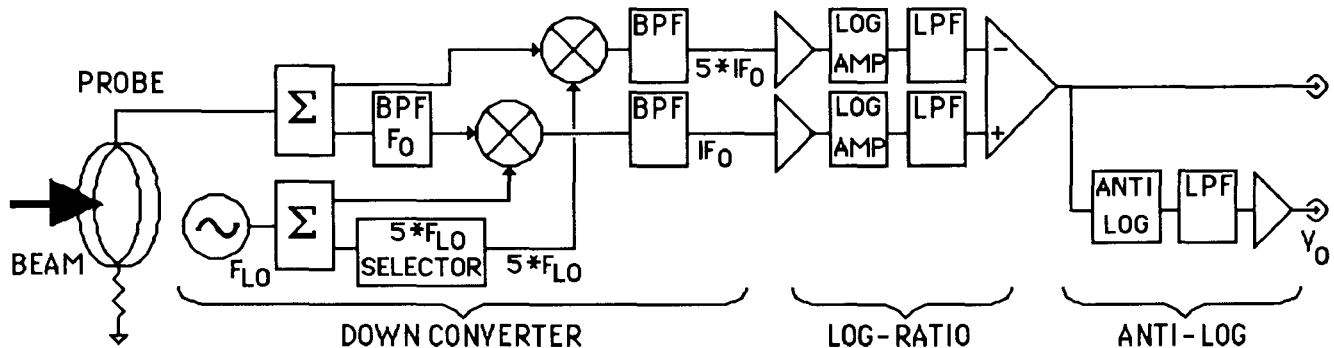


Fig. 2 The block diagram of the processing electronics shows how the fundamental and fourth-harmonic signal components from the probe are down converted to intermediate frequencies (IF_0 and $5X IF_0$), selected using bandpass (BPF) and low-pass (LPF) filters, and the log-ratio and antilogarithm functions are performed.

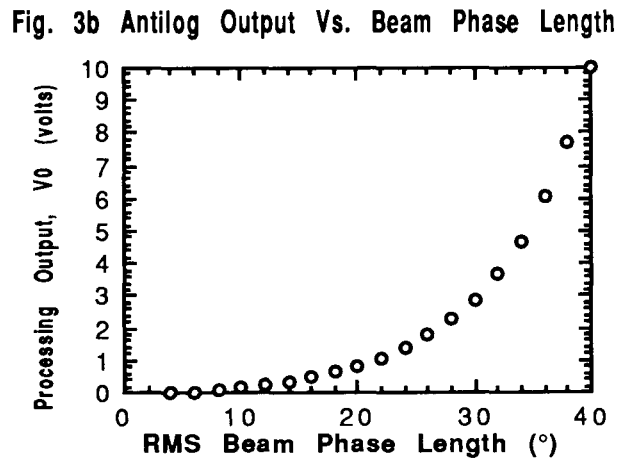
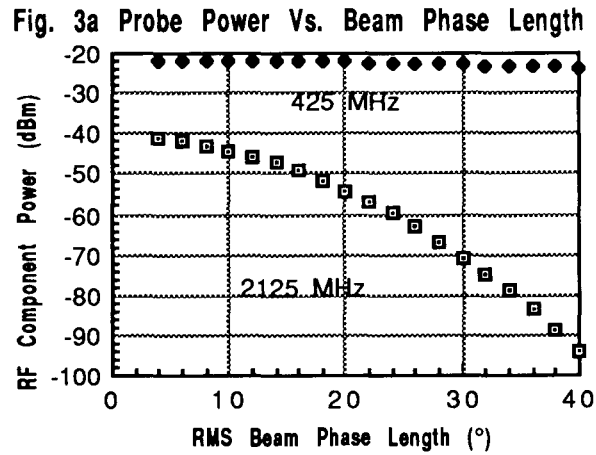


Fig. 3a & b These two graphs show the initial estimated input-signal power of the fundamental and fourth harmonic components and the antilogarithm output of the processing electronics as a function of rms beam bunch phase length.

Beam Distributions and Measurement Resolution

The ratio of the fundamental to higher-harmonic component amplitudes for a given rms length is relatively insensitive to changes in the beam bunch shape. For example, the fundamental and first four harmonic amplitudes agree to within approximately $\pm 5\%$ (i.e.,

equivalent ratio of ± 0.4 dB) for several different bunch shapes with a 10° rms length. However, in order to fully measure the longitudinal distribution, many higher-order harmonics must be measured [5]. The initial measurements were done using a Gaussian distribution in the signal power calculations and comparing only the rms phase lengths. Once this is completed, multiple harmonic measurements will be implemented.

One of the advantages of this measurement is that its rise time is approximately 5 μ sec, which implies a real-time bandwidth of 70 kHz. This is sufficiently responsive to measure the transient bunch length changes during the macropulse. The probe and electronics have a power-ratio resolution of ± 0.3 dB that is equivalent to an rms phase-length resolution of $\pm 2^\circ$. The ratio phase-spread monitor measures a beam phase spread of 5° to 40° over an operational beam-current range of 5 to 50 mA.

Measurement Results

Since the actual phase-spread distribution was unknown, a calibration of the ratio-based method was done by comparing its measured phase spread with that of the longitudinal emittance measurement. The comparison was done as a function of RFQ cavity power. The laser induced neutralization diagnostics approach (LINDA) accurately characterizes the beam's longitudinal phase space by neutralizing a few degrees of the bunch's phase distribution and then measures the energy spread of this neutralized bunch sample. Summarized in Fig. 4, the ratio and LINDA phase-spread data are plotted as a function of RFQ normalized cavity power.

Measured RMS Phase Spread Correlation

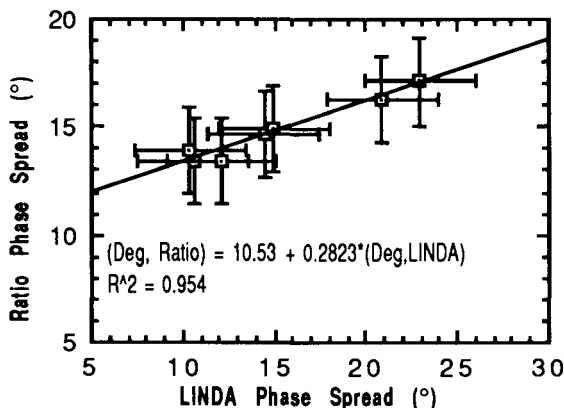


Fig. 4 LINDA and uncalibrated ratio phase-spread measurement data plotted as a function of the RFQ cavity power.

Since the LINDA technique measures the absolute longitudinal phase projection, it can be used to calibrate the ratio phase-spread measurement. Figure 5 correlates the LINDA and ratio phase-spread measurement data.

The 0.28 gain and 10.5° offset terms, respectively, as generated by a linear least-squares fit shown in Fig. 5, are the calibration for the ratio phase-spread monitor. These terms compensate for both the bunch shape and the initial errors in the estimates of signal power from the capacitive

probe. The well correlated fit, as notated by the " $R^2 = 0.954$ " value ($R^2 = 1.0$ describes the fit with the least squared error), is a verification that the two techniques track each other when changes occur in the beam phase spread. The error bars represent the absolute ($\pm 3^\circ$) and relative errors ($\pm 2^\circ$) for the particular LINDA and ratio phase-spread measurements.

Measured RMS Phase Spread Correlation

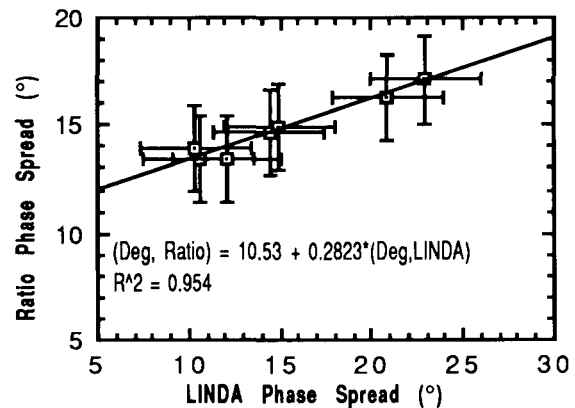


Fig. 5 Phase-spread measurement correlations between the LINDA and ratio phase-spread measurements. The linear fit's slope and offset for these data is the absolute calibration for the ratio phase-spread measurement.

Conclusions

The initial implementation and verification of the ratio phase-spread monitor has been completed. The ratio technique resolved phase-spread variations of less than $\pm 2^\circ$ and upon comparison with another phase-projection measurement was calibrated to within $\pm 3^\circ$. The capacitive probes provided the expected signal power for the 425- and 2125-MHz Fourier components for an operational phase-spread range of 5° to 40° . The processing-electronics' bandwidth is sufficiently wide to measure dynamic bunch-length variations within the beam macropulse. This technique will be extended for multiple harmonics which will improve both the phase-spread resolution and accuracy.

References

- [1] J. D. Gilpatrick, et al., "GTA Beam Diagnostics for Experiments 1B through 2D," Los Alamos National Laboratory document LA-UR-91-341.
- [2] V. W. Yuan, R. C. Connolly, R. Garcia, K. F. Johnson, K. Saadatmand, O. R. Sander, D. Sandoval, and M. Shinas, "Measurement of Longitudinal Phase Space in an Accelerated H-Beam Using a Laser-Induced Neutralization Method," (submitted to *NIM*).
- [3] R. E. Shafer, "Beam Position Monitoring," in *The Physics of Particle Accelerators*, AIP Conference Proceedings 249, Vol. 1, pp. 601-605.
- [4] J. H. Cuperus, "Monitoring of Particle Beams at High Frequencies," *NIM* **145**, 219-231 (1977).
- [5] K. Bongardt, K. Kennepohl, "Determination of 100 psec Short LINAC Bunches by Broadband Pickups and Reconstruction Techniques," in "Proceedings of EPAC Conference," (1988).